A runaway PRH/HHEX-Notch3 positive feedback loop drives cholangiocarcinoma and determines response to CDK4/6 inhibition.

Philip Kitchen[1], Ka Ying Lee[1], Danielle Clark[2], Nikki Lau[1], Jomnarong Lertsuwan[3], Anyaporn Sawasdichai[4], Jutamaad Satayavivad[4], Sebastian Oltean[5], Simon Afford[6], Kevin Gaston[7*#] and Padma-Sheela Jayaraman[1*#]

1. Institute of Cancer and Genomic Sciences, College of Medical and Dental Sciences, University of Birmingham, UK. 2.Department of Biochemistry, Medical School, University of Bristol, UK 3.Laboratory of Chemical Carcinogenesis, Chulabhorn Research Institute, Bangkok, Thailand; 4.Laboratory of Pharmacology, Chulabhorn Research Institute, Bangkok, Thailand; 5.Institute of Biomedical & Clinical Sciences, University of Exeter Medical School, Exeter, UK. 6.Institute of Immunology and Immunotherapy, University of Birmingham, Birmingham UK. 7.Division of Cancer and Stem Cells, School of Medicine, University of Nottingham, Nottingham, UK.

joint senior author and *joint corresponding author

Running title: PRH drives cholangiocarcinoma and chemotherapeutic response

7 figures

Email: p.jayaraman@bham.ac.uk tel. no. +44(0)121-414-4383

21 Email: kevin.gaston@nottingham.ac.uk tel. no. +44(0)115-8231395

22

23 **Declaration of Interests**

24 The authors declare no competing interests.

25

26

27

Abstract

Aberrant Notch and Wnt signalling are known drivers of cholangiocarcinoma (CCA) but the underlying factors that initiate and maintain these pathways are not known. Here we show that the PRH/HHEX transcription factor forms a positive transcriptional feedback loop with Notch3 that is critical in CCA. PRH/HHEX expression was elevated in CCA and depletion of PRH reduced CCA tumour growth in a xenograft model. Overexpression of PRH in primary human biliary epithelial cells was sufficient to increase cell proliferation and produce an invasive phenotype. Interrogation of the gene networks regulated by PRH and Notch3 revealed that unlike Notch3, PRH directly activated canonical Wnt signalling. These data indicate that hyperactivation of Notch and Wnt signalling is independent of the underlying mutational landscape and has a common origin in dysregulation of PRH. Moreover, they suggest new therapeutic options based on the dependence of specific Wnt, Notch, and CDK4/6 inhibitors on PRH activity.

Significance

The PRH/HHEX transcription factor is an oncogenic driver in cholangiocarcinoma that confers sensitivity to CDK4/6 inhibitors.

Keywords: cholangiocarcinoma, bile duct, biliary epithelial cells, cholangiocyte, HHEX, PRH, Notch, Wnt, epithelial-mesenchymal transition

Introduction

Cholangiocarcinoma (CCA) is a tumour of the bile duct epithelium with an unmet clinical need as this disease is usually advanced at diagnosis. For non-resectable disease median survival is less than 12 months and 5-year survival is around 2% (1). New treatment options and markers that allow early detection and/or inform personalised cancer treatment are therefore urgently needed. Risk factors for CCA include viral infection (Hepatitis B and C), liver fluke infection, primary sclerosing cholangitis (PSC), cholestasis (loss of bile flow), and exposure to dietary toxins or metabolites, all of which lead to inflammation in and around the biliary tree. Chronic inflammation can provoke uncontrolled wound-healing responses involving the generation of DNA-damaging reactive oxygen and nitrogen species, activation of immune cells (particularly macrophages) and stroma, and aberrant activation of autocrine signalling, as well as activation of signalling pathways that promote epithelial-mesenchymal transition (EMT) and angiogenesis. All these events ultimately lead to cancer development and progression (2). Many of the dysregulated pathways involved in CCA are also involved in embryonic liver morphogenesis, such as the Wnt, TGFβ, Notch, Hedgehog and Hippo pathways. Several of these pathways (including Wnt and Notch) can transiently promote EMT or the acquisition of mesenchymal features, such as increased cell migration and matrix invasion or loss of the epithelial cell-cell adhesion molecule E-cadherin (3, 4). In many cancers including mammary cancers, EMT is associated with an increased proportion of tumour initiating cells (the so-called cancer stem cells or CSC) that show increased self-renewal properties and increased chemoresistance (3). EMT and the CSC phenotype can be induced by any one of a common set of aberrantly expressed EMT transcription factors (e.g. Snail, Twist, Zeb) that, amongst many other things, directly repress the expression of E-cadherin (reviewed (5)). CCA patient samples exhibit decreased E-cadherin expression and contain CSCs (6) suggesting that EMT may also be a feature of CCA.

Canonical Wnt signalling is critical for cell proliferation and contributes to the development of CCA in a mouse CCA carcinogenesis model (7, 8). In canonical Wnt signaling, Wnt ligands activate Frizzled family receptors and stabilise the β-catenin protein which then enters the nucleus and activates transcription of Wnt target genes through interaction with TCF/LEF family transcription factors and co-activators (4). β-catenin, by acting as both a co-activator for TCF/LEF transcription factors and a structural component of adherens junctions *via* interaction with E-cadherin, facilitates cross-talk between canonical Wnt signalling and cell-cell adhesion. Although there are few mutations in Wnt signalling components in CCA there are high levels of nuclear β-catenin in the majority of CCA (7, 9). Importantly, pharmacological inhibition of Wnt signalling decreases CCA formation in mouse models (7).

NOTCH signalling is also of central importance to the development of CCA (10). Notch signalling involves four transmembrane NOTCH receptors and two families of ligands, Serrate/Jagged (JAG-1, -2) and Delta-like (DLL-1, -3, -4), along with other proteins that transduce and regulate the signal. Upon ligand binding, Notch receptors are sequentially cleaved by an ADAM family protease and the γ-secretase protease complex. Cleavage releases the NOTCH intracellular domain (ICD) which interacts with the DNA binding protein RBP-J/CSL and MAML1 co-activator resulting in transcriptional activation of NOTCH target genes, including the *HES* and *HEY* family of genes encoding bHLH transcriptional repressors (reviewed in (11)). In hepatic regeneration models, Wnt and Notch signalling promote different cell fates; Notch signalling promotes biliary fate in Hepatic Progenitor Cells and Wnt signalling promotes hepatic specification (12). Dysregulation of Notch signalling in mouse hepatocytes through constitutive Notch1 ICD or Notch2 ICD expression can result in either hepatocellular carcinoma (HCC) or CCA depending on the co-operating oncogene. *NOTCH3* is not expressed in adult liver but Notch3 expression is elevated in CCA patient samples and knockout of Notch3 in a mouse model of CCA

abrogates tumour growth (10). Notch3 ICD is known to be a key driver of CCA in part through activation of PI3K/Akt signalling (10). However, it is not known which genes the Notch3 ICD regulates nor is the interplay between Notch3 ICD signalling and Wnt signalling understood.

The Proline-Rich Homeodomain protein/Haematopoietically Expressed Homeobox (PRH/HHEX) protein is a transcription factor encoded by the *HHEX* gene that is required in the development of many tissue types including the liver and bile duct (reviewed (13)), where PRH regulates hepatic (HNF4a) and biliary (Onecut1) transcription factors, respectively (14). PRH plays a growth inhibitory role in hepatic regeneration (15) and when over-expressed in hepatocellular carcinoma cells PRH inhibited tumour growth in a mouse xenograft model (16, 17). PRH also exhibits tumour suppressive properties in other epithelial lineages and in some haematopoietic lineages (13). Similarly, in breast and prostate cells, PRH inhibits cell migration and loss or inactivation of PRH induces EMT-like changes in cell morphology and behaviour (18) and increases the proportion of CSC-like cells (19, 20). In stark contrast, PRH is involved in oncogenic transformation in at least two leukaemic subtypes in which cytogenetic rearrangements promote dysregulated PRH expression (21-23). As PRH potentiates Wnt signalling during early embryonic development (24) and early liver development (25) it is of interest to understand whether PRH plays a role in CCA and whether it is involved in regulating Wnt and Notch signalling .

Here we show for the first time that PRH plays an essential role in the maintenance of CCA. We also demonstrate that PRH promotes multiple features of tumour initiation and spread in primary untransformed biliary epithelial cells (cholangiocytes) isolated from human liver. Our work shows that a PRH-Notch3 positive feedback loop is a novel driver of CCA as both proteins collaborate to promote Wnt signalling. Further we demonstrate that PRH expression levels can determine sensitivity or resistance to novel CCA chemotherapeutic strategies.

Materials and methods

Cell culture and plasmids

CCLP-1, CCSW-1, AKN-1, KKU-100 and KKU-M213 cells (26, 27) were grown in Dulbecco's modified Eagle medium (DMEM) with L-glutamine (Sigma-Aldrich, D5796), supplemented with 10% FBS and MEM non-essential amino acids (Sigma-Aldrich, M1745). CCLP-1, CCSW-1, AKN-1 cells were authenticated in house by phenotyping using flow cytometry. KKU-100 and KKU-M213 (28) were obtained from the Japanese Cell Research Bank (JCRB1557 (KKU-213) and JCRB1568 (KKU-100)). HuCCA-1 (29) and RmCCA-1 (30) were kindly provided by the originators Prof. Stitaya Sirisinha and Assoc. Prof. Rutaiwan Tohtong respectively. HuCCA-1 and RmCCA-1 were grown in Ham's F12 medium (Thermofisher IBR21041025) and supplemented with 10% FBS. All cell lines were mycoplasma tested every 3 months using EZ-PCR mycoplasma test kit (Biological Industries). Primary biliary epithelial cells were isolated and grown as previously described (31). Stable cell lines were generated by transfecting PRH shRNA in pRS (Origene, TR312464), Notch3 shRNA in pLKO (Sigma-Aldrich, TRCN0000363316), CDH1 cDNA in pCDNA3 (hE-cadherin-pcDNA3 was a gift from Barry Gumbiner, Addgene plasmid #45769), or EGFP-PRH-myc in pEGFP-C1. Transient PRH knockdowns were performed using 100 nM each of 4 *HHEX* targeted siRNAs (Qiagen, 1027416). pEGFP-C1-PRH-Myc was generated by insertion of the human PRH cDNA between EcoRI and KpnI sites in pEGFP-C1. PCR was used to generate a PstI-KpnI fragment that replaced PRH coding sequence and placed an in-frame Myc tag followed by a translation stop codon at the end of the PRH coding sequence. This creates a double-tagged protein. Stable transfectants were selected for vector integration using either puromycin (pRS, pLKO) or G418 (pcDNA3, pEGFP-C1). For transient over-expression, PRH was over-expressed either using an

adenoviral construct at MOI 50, or using pMUG1-myc-PRH (32). For transient Rb knockdown we used 100nM of Rb targeted siRNAs (Qiagen, 1027416).

EdU incorporation

Cells were plated at 10^4 cells per well in 96-well plates, and EdU incorporation was measured after 24 hours. For inhibitor experiments, inhibitors were added at the time of plating. Click-It EdU microplate kit (ThermoFisher, C10214) was used according to the manufacturer's instructions with the exception of replacement of the fluorescent kit substrate with the colourimetric peroxidase substrate o-Phenylinediamine (Sigma-Aldrich, P9187) to improve signal:noise. Cell lines were incubated with EdU for 2 hours and primary cells for 4 hours.

Immunohistochemistry

A formalin-fixed paraffin embedded cholangiocarcinoma tissue microarray (TMA) was purchased from Abcam (ab178201). Antigen retrieval was performed using 10 mM citrate, 0.05% tween-20, pH 6.0 in a microwave on full power (800 W) for 30 minutes. The array was stained using an in-house polyclonal mouse anti-PRH antibody and the Vector ImmPRESS kit (Vector labs, MP-7402), and imaged on a Zeiss Axio Scan.Z1 microscope.

Immunocytochemistry

Cells were seeded onto poly-L-lysine-coated glass coverslips and left to adhere for 24 hours. Cells were washed with PBS and fixed using 4% formaldehyde in PBS for 10 minutes. Cells were permeabilized using 0.1% Triton X-100 in PBS for 10 minutes then blocked in 5% BSA + 20% serum from the secondary antibody host species in PBS. Primary antibodies used were E-cadherin (Cell Signaling Technology, 24E10) and β-catenin (Cell Signaling Technology, D10A8). Secondary antibody was Texas Red conjugated anti-rabbit IgG (Sigma-Aldrich,

SAB3700873). Cells were mounted using Prolong Gold with DAPI (ThermoFisher, P36931), and imaged using a Zeiss LSM 780 confocal microscope.

Western blotting

The following primary antibodies were used for Western blotting: PRH (in-house mouse polyclonal (33)), E-cadherin (Cell Signaling Technology, 24E10), Lamin A/C (Santa Cruz, H-110), myc tag (Cell Signaling Technology, 9B11), Notch3 (Cell Signaling Technology, D11B8), Vimentin (Cell Signaling Technology, D21H3), Cyclin D2 (Cell Signaling Technology, D52F9), Rb (Cell signalling Technology, 4H1), Phospho-Rb (Ser807/811) (Cell signalling Technology, 9308).

Quantitative RT-PCR

RNA was extracted using a Bioline Isolate II kit according to the manufacturer's instructions. 1μg of total RNA was used for reverse transcription (Quantitect Reverse Transcription kit (Qiagen, 205311)). qRT-PCR was performed in a Rotor-Gene Q cycler (Qiagen) using Quantitect SYBR green PCR kit (Qiagen, 204143). Genes of interest were normalised to β-actin expression using primer efficiency normalised relative quantification, with primer efficiencies calculated from standard curves generated from cDNA dilutions. All primers are listed in supplementary table 1.

Mouse xenografts

All animal experiments and procedures were approved by the UK Home Office in accordance with the Animals (Scientific Procedures) Act 1986, and the Guide for the Care and Use of Laboratory Animals was followed. 10^6 CCLP-1 PRH knockdown or scrambled control cells were resuspended in 100 μL Matrigel and injected subcutaneously into the flank of male CD-

1 nude mice. Tumours were measured with a calliper every three days until the tumour reached 12 mm in diameter. Tumour volume was estimated using the following formula: [(length+width)/2]*length*width.

RNA sequencing

RNA was isolated using a Bioline Isolate II kit according to the manufacturer's instructions. Total poly-adenylated RNA was purified and adapter ligated using Illumina TruSeq RNA Library Prep kit according to the manufacturer's instructions. This was followed by Illumina sequencing of 75bp paired end reads (minimum 2x35 million reads/sample). Each experimental condition was run in biological duplicate. Reads were quality-trimmed using TrimGalore!, aligned using the gapped read mapper TopHat and differential expression analysis was performed using DESeq2. Gene Ontology analysis was performed using the PANTHER webserver (http://www.pantherdb.org) and Gene Set Enrichment Analysis for Hallmark gene sets was performed using the Broad Institute GSEA webserver (http://software.broadinstitute.org/gsea/msigdb). Raw and processed RNA-seq data has been submitted to NCBI GEO database Accession no. GSE124429.

ChIP sequencing

CCLP1 cells were infected with a recombinant adenovirus to express myc-PRH. Chromatin immunoprecipitation of myc-PRH (using the same antibody as for myc-tag Western blots) was carried out as previously described (34) with 1.5×10^7 CCLP1 cells infected with Ad-myc-PRH or empty adenovirus at MOI 50 for 48hrs. Sequencing libraries were prepared using NEBNext Ultra II DNA Library preparation kit, followed by Illumina sequencing of 100bp reads (minimum 20 million reads/sample). Reads were quality-trimmed using TrimGalore!, aligned using Bowtie2 and peaks were called using MACS2. Chromatin

prepared from empty adenovirus infected cells and subjected to myc tag immunoprecipitation was used as background in sequencing and peak calling. *De novo* motif analysis of ChIP peaks was performed using HOMER. Raw and processed ChIP-seq data has been submitted to NCBI GEO database Accession no. GSE124430.

TCF/LEF reporters

TCF/LEF dependent transcriptional activity was measured using the TOPflash firefly luciferase reporter system, in which the firefly luciferase gene is downstream of several TCF/LEF consensus binding sites; the same construct with scrambled TCF/LEF sites (FOPflash) is used to determine the TCF/LEF-independent activity of the promoter. Firefly luciferase activity was normalised to *Renilla* luciferase activity from a constitutively active promoter (pRL, Promega, E2261). For over-expression experiments, reporter constructs were co-transfected with either myc-PRH, myc-PRH N187A DNA-binding deficient mutant (32) or 3xFLAG-Notch3-ICD (hNICD3(3xFLAG)-pCDF1-MCS2-EF1-copGFP, a gift from Brenda Lilly, Addgene plasmid #40640) expression vectors.

Soft agar colony formation

Colony formation assays and subsequent imaging were done as described by Borowicz et al (35). 10^3 cells were plated per well and colonies were imaged after 10 days.

Transwell migration

Cells were starved overnight in serum-free medium with 0.2% BSA and 1mM hydroxyurea. 24 well ThinCert inserts (Greiner bio-one) were placed in the wells of a 24 well plate. 600µL DMEM with 10% serum was added to each. 200 µL of serum-free medium with 0.2% BSA containing $2x10^5$ cells was added to each insert. After 72 hours medium was replaced with

450 µL of 8 µM calcein-AM in DMEM with 10% serum. After 45 minutes incubation, inserts were transferred to a fresh 24 well plate containing 500 µL prewarmed Trypsin-EDTA in each well. 200 µL of the Trypsin-EDTA cell suspension was transferred to a black flat bottom 96 well plate. The fluorescence signal was read in a fluorescence plate reader at an excitation wavelength of 485 nm and an emission wavelength of 520 nm.

Matrigel invasion

For invasion assays, insert transwells with 8.0 µm polycarbonate membrane (Corning costar, New York, NY, USA) were coated with 50 µl of a 1:10 mixture of Matrigel™ (BDBiosciences, San Jose, CA, USA) in serum free medium. Cells were infected with Ad-empty or Ad-PRH (moi 50) and 24 hours after infection cells incubated with 1mM hydroxyurea. 48 hours after infection 10^4 cells were plated per well in serum free media containing 1mM hydroxyurea (200ul) and left to invade towards complete medium (500ul) in the bottom chamber for 24 hours. Cells remaining on underside of insert after swabbing with a cotton swab were fixed in methanol for 5 mins and stained with 0.1%w/v crystal violet in 12% glutaraldehyde in water for 5 mins and counted by microscopy.

Results

PRH is highly expressed in CCA.

Analysis of the cholangiocarcinoma dataset (n=45) in The Cancer Genome Atlas (TCGA) revealed elevated expression of PRH mRNA in CCA samples compared to all TCGA samples, with a mean $\log_2$ fold-change of 3.2±0.9 (Fig.S1A) and high PRH expression is limited to a small number of tumour types (Fig.S1B). In the majority of CCA samples, elevated PRH mRNA expression is in the absence of gene amplification and in several samples the transcript is elevated despite a single allele deletion. No coding mutations in the *HHEX* gene encoding PRH were detected in any CCA samples. To examine PRH protein staining intensity in CCA samples we performed immunohistochemistry on a tissue microarray containing 2 tumour cores and a non-involved border core from 42 CCA patients (Abcam). Representative immunohistochemistry images of carcinomas and patient-matched border bile ducts are shown in Fig.1A. Of the 42 non-involved border cores, 26 had at least one bile duct. In a paired analysis of these 26 samples compared to their matched carcinoma, we found increased PRH staining intensity in 20/26 (p=0.00005), and in an unpaired analysis comparing all 42 carcinomas to the 26 non-involved bile ducts we found a 20% increase in median PRH expression (p=0.0004, Fig.1B). We did not find any differences in PRH staining intensity between different grades or TNM stages of carcinoma, although this may reflect lack of statistical power as the majority of our samples were from grade II tumours. We next examined PRH protein expression in four CCA cell lines compared to immortalised AKN-1 biliary epithelial cells (BECs) and two independently isolated primary human BEC cultures derived from livers with alcoholic liver disease (ALD) and steatotic liver disease (NASH). All four CCA cell lines showed increased PRH protein expression (Fig.1C) and we conclude that PRH mRNA and protein is highly expressed in CCA compared to primary BECs.

PRH promotes tumour growth by CCLP1 cells in nude mice.

To determine whether elevated PRH is important in CCA we generated stable PRH knockdown (KD) in CCLP1 CCA cells. Western blotting and quantitative RT-PCR demonstrated effective knockdown of PRH (Fig.S1C and S1D). One million CCLP1 control and PRH knockdown cells were then injected subcutaneously into nude mice and tumour size measured over 25 days and at the termination of the experiment. Only 3/9 mice injected with PRH knockdown cells produced tumours compared to 9/9 controls (p=0.003) and knockdown of PRH expression significantly reduced tumour growth (Fig.1D). PRH knockdown also reduced the proportion of CCLP1 cells able to form colonies in soft agar (Fig.1E) and the average colony cross-sectional area (Fig.1F). To test whether over-expression of PRH in BECs would be sufficient to recapitulate the phenotype observed in CCLP1 cells, AKN1 immortalised BECs were transfected with a double-tagged GFP-PRH-myc expression vector and selected to generate a stable GFP-PRH-myc expressing cell line. In addition we over-expressed PRH in primary BECs using an adenovirus expressing myc-tagged PRH. Colony formation in soft agar was increased in an AKN1 cell population over-expressing PRH compared to controls (Fig.1G-H) and strikingly, when expressing myc-PRH multiple independently isolated primary BEC populations from different donors were able to form colonies in soft agar whereas controls were not (Fig.1I). We conclude that elevated PRH expression promotes anchorage-independent growth of primary and immortalised BECs *in vitro* and that reduction of PRH levels inhibits CCLP1 tumour growth in a xenograft model.

PRH drives CCA cell proliferation.

To examine why depletion of PRH in CCA cells decreases tumour growth in nude mice we examined the effect of PRH depletion and PRH over-expression on cell proliferation in culture. Knockdown of PRH in CCLP1 cells reduced cell growth, with the doubling time

316 increasing from 28±3 to 40±4 hours (Fig.S1E). To determine whether this was due to reduced
317 proliferation or increased cell death we measured proliferation by EdU incorporation and
318 apoptosis by caspase-3 enzymatic activity assay. EdU incorporation was reduced to 53±7%
319 of control with PRH shRNA knockdown (Fig.2A). There was a small decrease in caspase-3
320 activity in PRH knockdown cells compared to controls (Fig.S1F). We conclude that the
321 reduction in cell number on PRH knockdown was predominantly a result of decreased cell
322 proliferation. To determine whether this was a CCLP1-specific effect, or an off target effect
323 of the PRH shRNA, we also measured EdU incorporation in KKU-M055 and KKU-M213
324 CCA cells 72 hours after transfection with a PRH siRNA with a different target sequence to
325 the shRNA. EdU incorporation was reduced in both cell types (Fig.S1G) ruling out cell line-
326 specific effects and off-target effects of the shRNA. To confirm that PRH promotes the
327 proliferation of CCA cells we over-expressed PRH in CCLP1 and CCSW1 CCA cells using a
328 recombinant adenovirus encoding myc-PRH (Fig.S2A). Over-expression of myc-PRH in both
329 cell lines increased EdU incorporation (Fig.2B) and increased growth rate, with doubling
330 times decreased from 30±3 to 22±1 hours and 29±4 to 19±3 hours, respectively (Fig.S2B).
331 Caspase-3 activity was also robustly decreased (Fig.S2C). Proliferation measured by EdU
332 incorporation was increased by PRH over-expression in both primary BECs and AKN1 cells
333 (Fig.2C). We conclude that PRH over-expression promotes the proliferation of primary BECs
334 and CCA cell lines and reduces basal levels of apoptosis.
335
336 *PRH maintains the mesenchymal phenotype of CCA cells.*
337 Following PRH knockdown in culture we noticed a marked change in morphology of CCLP1
338 cells from an elongated mesenchymal-like morphology to an epithelial-like morphology
339 (Fig.2D). Unlike normal BECs, CCLP1 cells do not express the epithelial cell adhesion
340 molecule E-cadherin. However, E-cadherin expression was restored upon PRH knockdown

(Fig.2E) and the mesenchymal marker protein Vimentin was also strongly decreased in these cells (Fig.2E, lower). As changes in cell morphology and E-Cadherin expression are associated with mesenchymal to epithelial transition (MET) we measured the migration and invasion of PRH depleted CCLP1 cells in response to a serum gradient. Proliferation was inhibited by hydroxyurea treatment in both experiments. PRH knockdown reduced the number of migrated cells (Fig.2F) and reduced the number of invaded cells (Fig.2G). Overexpression of PRH in the presence of hydroxyurea increased the invasion of both CCLP1 and CCSW tumour cell lines (Fig.S2D). Over-expression of PRH in both AKN1 and primary human BECs reduced E-Cadherin expression and increased expression of Vimentin (Fig.2H). In addition, PRH over-expression increased cell migration and matrix invasion by both primary BECs and AKN1 cells (Fig.2I-J). As might be expected based on these results, PRH expression in AKN1 cells resulted in a change from an epithelial-like cell morphology to a more mesenchymal cell morphology (Fig.2K). We therefore examined changes in the expression of EMT-related genes in AKN1 cells over-expressing PRH using qRT-PCR. The epithelial and mesenchymal marker genes *CDH1* and *VIM* encoding E-Cadherin and Vimentin were down-regulated and upregulated respectively, following PRH expression (Fig.S2E). In addition, the genes encoding EMT transcription factors (*ZEB1*, *TWIST1*) were upregulated in AKN1 cells expressing PRH. Thus PRH over-expression in primary BECs and in an immortalised BEC cell lines supresses the epithelial phenotype and promotes a migratory mesenchymal phenotype.

PRH regulates pathways associated with Wnt signalling and with EMT.

To understand how PRH promotes the proliferation of CCA cells and maintains a mesenchymal phenotype, we performed RNA sequencing (RNA-seq) with total poly-adenylated RNA isolated from CCLP1 cells with stably knocked down or transiently over-

366 expressed PRH. We found 189 down-regulated and 430 up-regulated genes in PRH
367 knockdown cells, and 889 down-regulated and 1410 up-regulated genes in PRH over-
368 expressing cells when compared to their respective controls (Fig.3A). To validate the RNA-
369 seq data, we performed qRT-PCR for several genes identified as differentially expressed, all
370 of which were in agreement with the RNA-seq (Fig.S3A). Gene Set Enrichment Analysis
371 (GSEA) using the Molecular Signatures Database (MSigDB) Hallmark gene sets (36) showed
372 that both PRH knockdown and PRH over-expression led to the differential expression of
373 genes within the same pathways many of which have been shown to be aberrantly activated
374 in CCA including EMT, Wnt/β-catenin, TGF-β, IL6/JAK/STAT3 and estrogen signalling
375 (Fig.3B and Fig.3C). Gene Ontology (GO) term enrichment analysis was in broad agreement
376 with GSEA analysis and suggested enrichment of genes associated with epithelial and
377 mesenchymal differentiation as well as genes associated with both canonical and non-
378 canonical Wnt signalling (Fig.S3B and S3C). We also noted changes in the expression of
379 multiple transcription factors and markers associated with biliary differentiation and Notch
380 signalling (Fig.3D). These results are suggestive of alteration of the transcriptional network
381 underlying biliary differentiation upon PRH knockdown.
382 In addition, GO analysis identified enrichment of genes associated with the control of cell
383 proliferation in both the knockdown and over-expression experiments, including genes
384 encoding cyclin D2 (*CCND2)*, and the p27 (*CDKN1B*) and p15 (*CDKN2B*) cyclin-dependent
385 kinase (CDK) inhibitors (Fig.S3B and Fig.S3C), and GSEA analysis showed enrichment of
386 the G2M gene set which contains cell cycle genes (Fig.S3C). Of particular interest in the
387 GSEA data was the finding that Notch and PI3K/Akt pathway genes were enriched in the
388 PRH over-expression gene set (Fig.3C) as *NOTCH3* oncogenic activity in CCA models is at
389 least partly due to non-canonical NOTCH signalling via PI3K/Akt (10). Furthermore, the
390 *NOTCH3* gene was one of the 53 genes that were differentially regulated in both PRH over-

391 expression and knockdown data sets, and both qRT-PCR and Western blotting showed
392 reduced *NOTCH3* gene expression and Notch3 ICD protein expression in PRH knockdown
393 cells (Fig.3D and 4A, respectively).

394 *A PRH-Notch3 positive feedback loop promotes cell proliferation and EMT.*

395 To determine whether NOTCH3 expression was increased by PRH in other CCA cell lines
396 we over-expressed myc-PRH and a DNA binding deficient myc-PRH N187A mutant in
397 CCLP1 and CCSW1 cells. Wild-type PRH but not the DNA binding deficient mutant
398 increased *NOTCH3* mRNA (Fig.4B) and protein levels in these cells (Fig.4C). Furthermore,
399 we found a striking correlation between PRH expression and Notch3 expression in cell lines
400 and primary BECs (Fig.4D). In addition, *HHEX* and *NOTCH3* gene expression positively
401 correlated in the TCGA CCA RNA-seq dataset as do *HHEX* and *HES1* gene expression
402 (Fig.S3D and S3E), suggesting that PRH regulates *NOTCH3* and *HES1* in primary tumours.
403 Finally, over-expression of PRH in both primary BECs and AKN1 cells led to expression of
404 the Notch3 protein (Fig.4E).

405 To determine whether the effects of PRH knockdown are recapitulated by depletion of
406 Notch3, we generated Notch3 knockdown CCLP1 cells by integrating a Notch3 shRNA
407 plasmid (Fig.4F). Strikingly, the proliferative and morphological phenotype of PRH
408 knockdown cells (Fig.2A and 2D) was reproduced by Notch3 knockdown (Fig.4F-H).
409 Moreover, knockdown of Notch3 resulted in a reduction of *HHEX* mRNA (Fig.S3F) and
410 PRH protein (Fig.4F). These data suggest that PRH and Notch3 could form a positive
411 transcriptional feedback loop where each regulates the other.

412 To better understand the transcriptome changes underlying the common phenotype between
413 Notch3 and PRH knockdown cell lines, we performed RNA-seq with Notch3 knockdown and
414 scrambled shRNA cell lines and compared differentially expressed genes (DEGs) in PRH
415 knockdown cells to those in Notch3 knockdown cells. These experiments clearly showed that

both factors act in the same pathways as the DEGs after PRH depletion were a subset of those differentially expressed after Notch3 knockdown (see Venn diagrams, Fig.4I). In agreement with this finding, the gene sets enriched in the Notch3 knockdown DEGs were largely the same sets enriched in PRH knockdown (red bars, Fig.4J), with a small number of Notch3-specific sets (black bars) including PI3K/Akt signalling and Notch signalling. In agreement with the GSEA, Western blotting experiments showed that both PRH knockdown and Notch3 knockdown reduced phosphorylation of Akt at both T308 and S473 (both of which are known to increase kinase activity, T308 by 100-fold and S473 by a further 10-fold for full kinase activity (37)) (Fig.S3G).

Notch3-dependent and Notch3-independent PRH target genes.

To separate PRH-regulated genes into Notch3-dependent (Notch correlated) and Notch3-independent (PRH correlated) subgroups, we over-expressed PRH in Notch3 knockdown CCLP1 cells. Figure 5A shows qRT-PCR analyses examining representative PRH-correlated and Notch3-correlated genes. Expression of the PRH regulated EMT associated genes *CDH1* and *VIM*, as well as *CCND2* was regulated by Notch3 rather than by PRH alone and this result was reproduced at protein level (Fig.5B). EdU incorporation experiments after over-expression of PRH in Notch3 knockdown cells suggested that PRH was unable to drive proliferation when it was decoupled from activation of Notch3 expression (Fig.5C). Interestingly, we noted a reduced level of PRH mRNA and protein expression from the adenoviral PRH construct in the Notch3 knockdown cells compared to the control (Fig.5A and Fig.5B) suggesting that Notch3 may regulate PRH expression at the level of transcript stability. We found the same effects on proliferation and expression of genes and proteins shown in Fig.5A/B when the viral MOI was increased in the Notch3 knockdown cells to give equal PRH protein expression and we therefore proceeded to perform RNA-seq in the

presence of equal MOIs. Across all four sample combinations, we found 5397 DEGs which were correlated with either PRH or Notch3 expression. Of these, 4356 were Notch3-correlated (2110 positively correlated i.e. activated downstream of Notch3, and 2246 negatively correlated i.e. repressed downstream of Notch3), and 1041 were PRH-correlated (604 positively and 437 negatively)(Fig.5D). We found strong enrichment of c-myc target genes when we performed GSEA analysis on the 1041 PRH correlated genes (Fig.5D lower panel). In addition to c-myc target genes, we found enrichment of a variety of gene sets (including Wnt/β-catenin signalling) that are also enriched in the Notch3-correlated gene set, suggesting that PRH and Notch3 regulate different genes in the same pathways (Fig.5D). Finally, we present summary heat maps with hierarchical clustering analysis of all RNA-seq samples showing PRH dependence, Notch dependence or co-dependence of genes (Fig.S4A) and heat maps with hierarchical clustering analysis of RNA-seq samples for selected pathways (Fig.S4B).

Identification of PRH binding sites in CCA cells.

To identify putative direct targets of PRH, we determined the genome-wide binding sites of PRH in CCLP1 cells using chromatin immunoprecipitation sequencing (ChIP-seq) with a myc-tag antibody and chromatin prepared from myc-PRH or empty adenovirus infected CCLP1 cells and assigned ChIP peaks to the nearest transcription start site within 100kb. Comparison of these putative direct PRH target genes with the DEGs from the myc-PRH over-expression RNA-seq experiment suggests that of the 1410 up-regulated genes, only 143 (10.1%) were direct targets, whereas of the 889 down-regulated genes, 397 (44.7%) were direct PRH targets (see Venn diagram, Fig.5E). These data produced the first consensus binding site identified for PRH in cells (Fig.5F); the most strongly enriched motif (64.2% of peaks, $p=10^{-96}$) underlying PRH ChIP-seq peaks contains a core ATTA motif characteristic of

homeodomain transcription factor binding sites (Fig.5F) and is in good agreement with the avian PRH binding site determined *in vitro* by SELEX (38). Variants of this sequence have been identified upstream of several PRH regulated genes in other cell types (39). Analysis of the putative directly regulated genes using GSEA, revealed enrichment of genes associated with apoptosis, proliferation (mitotic spindle and G2M checkpoint), EMT, and signalling pathways including IL6, IL2, p53 and TNF-α (Fig.S5A). Multiple genes associated with EMT including genes involved in cell adhesion or cell migration were present in these groups, however these targets do not include the *SNAI*/*TWIST*/*ZEB* families of EMT transcription factors that regulate *CDH1* or *CDH1* itself. PRH did not directly bind near *NOTCH3* and thus PRH may regulate Notch pathway genes by indirect means. However, *CDKN1B* and *CDKN2B* genes (Fig.S5B and Fig.S5C) and a number of genes associated with Wnt signalling including *DKK1, WNT11* (Fig.5G and Fig.5H), *TCF7L1* and *WNT16* had nearby PRH ChIP peaks.

Notch3-dependent and Notch3-independent effects on Wnt signalling.

To determine whether PRH regulates Wnt signalling in these cells, we made use of the TOPFlash TCF/LEF luciferase Wnt-signalling reporter system (40). Transient transfection of plasmids encoding myc-PRH into both CCLP1 and CCSW1 cells significantly increased TOPFlash activity compared to the empty vector control (Fig.6A) or after over-expression of the DNA-binding deficient N187A PRH mutant (Fig.6A, inset). Transfection of FLAG-Notch3-ICD did not alter the activity of the TOPFlash reporter (Fig.6A) despite robust protein expression (Fig.S3H) and changes in the expression of Notch3 target genes (*HEY2* and *CCND2,* Fig.S3I). This suggests that genes directly downstream of PRH rather than genes regulated by Notch3 are crucial for controlling the output of the canonical Wnt signalling pathway in these cells.

β-catenin facilitates cross-talk between canonical Wnt signalling and cell-cell adhesion by acting as a co-activator for TCF/LEF transcription factors and a structural component of the adherens junctions complex that includes E-cadherin (41). Although there was no change of β-catenin gene expression after PRH over-expression or knockdown, we observed a large increase in E-cadherin expression after PRH knockdown in CCLP1 cells (Fig.2E) and decreased E-cadherin expression after PRH over-expression in BECs (Fig.2H). PRH knockdown reduced β-catenin nuclear localization compared to the control as measured by immunofluorescence micrographs (Fig.6B) and densitometry of Western blots for β-catenin following subcellular fractionation (Fig.6C). TCF/LEF reporter activity in PRH knockdown CCLP1 cells was also decreased (Fig.6D). To determine whether the increased expression of E-cadherin could explain the reduction in TCF/LEF transcriptional activity in PRH KD cells, we restored E-cadherin protein expression independently of EMT transcription factors in CCLP1 cells by generating a stable cell line expressing the *CDH1* gene under the control of the CMV promoter. Expression of E-cadherin decreased TOPFlash reporter activity (CDH1 empty TOP compared to pcDNA empty TOP in Fig.6E), suggesting that the increase in E-cadherin seen on PRH depletion (and consequent decrease in β-catenin nuclear localisation) is likely to be responsible for decreased Wnt signalling. Moreover, E-cadherin over-expression significantly reduced the ability of PRH to increase TOPFlash reporter activity (Fig.6E). Taken together, these data indicate that PRH directly promotes aberrant expression of Wnt pathway genes leading to activation of Wnt-responsive transcription independently of Notch3. In addition, repression of *CDH1* downstream of PRH via Notch3 amplifies the aberrant PRH-dependent Wnt signal. Thus PRH and Notch3 exert regulation over Wnt signalling at multiple levels.

PRH over-expression and sensitivity to chemotherapeutic drugs.

As PRH regulated several components of the Notch signalling pathway including γ-secretase components, we investigated whether PRH could modulate the inhibition of cell proliferation by γ-secretase inhibition. Treatment with the γ-secretase inhibitor DAPT had a greater inhibitory effect on the proliferation of CCLP1 cells than it did on the proliferation of CCLP1 cells over-expressing PRH (Fig.7A). To summarise these data we calculated a log ratio of sensitivity between CCLP1 and PRH over-expressing CCLP1, as $\log_2((P_{PRH,drug}/P_{PRH,vehicle})/(P_{empty,drug}/P_{empty,vehicle}))$ where *P* is the relative proliferative rate measured by EdU incorporation (Fig.7B). The log ratio is negative if PRH expression increases sensitivity to a drug, and positive if it increases resistance. PRH also drives canonical Wnt signalling in CCA cell lines, and we wondered whether the anti-proliferative effect of Wnt pathway inhibition previously reported in CCA cell lines (7) would be modulated by the PRH expression level. Treatment with the β-catenin/CBP interaction inhibitor ICG-001 had a greater inhibitory effect on the proliferation of CCLP1 cells than it did on the proliferation CCLP1 cells over-expressing PRH (Fig.7A/7B and dose-response curve Fig.S6A). These data indicate that high PRH levels induce resistance to canonical Wnt pathway inhibition by ICG-001 as well as resistance to γ-secretase inhibition. It has recently been shown in a mouse model of AML that repression of *Cdkn2a* by PRH is dependent on recruitment of Polycomb repressive complex 2 (PRC2) (23). We therefore tested whether inhibition of EZH2, the catalytic subunit of PRC2 (using UNC1999), would block proliferation of CCLP1 cells in a PRH-dependent fashion. However, although EZH2 inhibition reduced cell proliferation, the effect was PRH-independent (Fig.7A/7B).

Since exogenous PRH represses *CDKN1B* and *CDKN2B* and activates *CCND2* indirectly via Notch3 we next examined whether inhibition of CDK4/6 using palbociclib would block proliferation in CCLP1 cells and whether sensitivity to this drug is modulated by PRH expression level. EdU incorporation experiments with CCLP1 cells over-expressing PRH in

the presence of palbociclib showed that high levels of PRH sensitised CCLP1 cells to the anti-proliferative effects of palbociclib (Fig.7A/7B and dose-response curve Fig.S6B). We conclude that PRH over-expression drives CDK4/6 activity via both increased expression of cyclin D2 (via Notch3) and by direct repression of p15 and p27 expression. To determine whether increased PRH levels result in increased sensitivity to palbociclib in other CCA cell lines, we over-expressed the protein in a panel of cell lines in the presence of palbociclib and measured EdU incorporation. Figure 7C shows the log ratio of sensitivity between control cells and PRH over-expressing cells in each case. In all of the cell lines tested increased PRH levels result in increased sensitivity to palbociclib treatment.

The effect of palbociclib on cell proliferation is thought to be dependent on the presence and inhibition of phosphorylation of the Rb tumour suppressor protein (42). We therefore examined Rb expression in the CCA cell lines and BECs used in this study. Interestingly, Rb protein expression was very low or not detectable in primary BECs or immortalised BECs although it is present in CCA cell lines (Fig.S7A). Moreover, treatment of CCA cell lines with palbociclib at their LD50 reduced the levels of phosphorylated Rb in each case (Fig.S7B). To determine whether the effects of palbociclib on the proliferation of CCLP1 cells requires the presence of Rb we knocked down Rb using siRNA. Although the proliferation of control cells was inhibited by palbociclib treatment, Rb knockdown CCLP1 cells are far less sensitive to the effects of this drug (Fig.7D). In addition, palbociclib has no effect on the proliferation of PRH knockdown CCLP1 cells (Fig.7D).

Figure 7E summarises the transcriptome and phenotypic changes that are dependent on PRH expression and the associated altered sensitivities to palbociclib and other chemotherapeutics. We conclude that the clinical efficacy of various chemotherapeutic strategies is likely to depend on PRH expression level, and that patient stratification on the basis of PRH

565 expression could improve the clinical usefulness of several compounds that have recently
566 been suggested as potential novel CCA treatments including palbociclib.
567

Discussion

Previous work in a variety of animal and *in vitro* models has suggested that hyper-activation of both Wnt signalling (7) and Notch signalling (10) are crucial events in carcinogenesis and progression of CCA. Here we show that both of these events have a common origin in the dysregulation of PRH. We reveal that the PRH protein is elevated in human CCA cell lines and primary tumours relative to primary BECs and we use a xenograft model and colony formation assays with primary human biliary epithelial cells to demonstrate the importance of PRH in CCA. We show that PRH depletion in CCA cells decreases cell proliferation and inhibits cell migration and cell invasion and brings about changes in gene expression consistent with MET. The ability of PRH to influence tumour cell behaviour is not confined to increasing cell proliferation and maintaining a mesenchymal phenotype in CCA cell lines. Indeed over-expression of PRH increases cell proliferation, migration, invasion and anchorage independent growth of primary human BECs and AKN1 cells. Moreover transient elevated PRH expression in primary BECs induces changes in gene expression characteristic of EMT. Collectively these experiments show that PRH is a novel oncoprotein in at least a large proportion of CCA tumours and they suggest that PRH dysregulation underlies both CCA and the biliary pathologies that precede CCA.

PRH regulates NOTCH3 in CCA

We have shown that PRH is a regulator of *NOTCH3* gene expression. However, ChIP-seq experiments did not show binding of PRH near *NOTCH3* or near to any of the other PRH-regulated genes in the Notch pathway, such as *NOTCH1*, *JAG1* and *JAG2*. Although the regulation of *NOTCH3* appears to be indirect, it is one of only 53 genes that are differentially expressed upon both over-expression and knockdown of PRH. We also show that *NOTCH3* knockdown decreases PRH expression and that this creates a positive feedback loop. One

consequence of activation of a Notch3-PRH positive reinforcement loop in CCA and in primary BECs is that a small perturbation to the activity or expression of either factor could lead to amplification of gene expression changes that ultimately give rise to the phenotypic alterations associated with CCA. Since we observed a strong correlation between *HHEX* and *NOTCH3* gene expression in the whole TCGA dataset, which contains samples with a variety of driver mutations, we propose that a positive feedback loop between Notch3 and PRH is initiated independently of the underlying mutational landscape through common changes in the tumour microenvironment and the intracellular signalling milieu. We also see correlation of *HHEX* and *HES1mRNA expression* which may occur because of co-regulation of *HES1* by PRH and Notch3. The co-activation of multiple genes in the pathway such as the gamma secretase activator *PSEN2* by Notch3 and PRH likely also leads to the increase in Notch3 ICD observed following PRH expression.

Previous studies showed that Notch3 promotes PI3K/Akt signalling in CCLP1 cells in a non-canonical manner (10). Here we present the first genome-wide identification of Notch3 regulated genes in CCA and we use GSEA to show that multiple PI3K/Akt/mTOR pathway genes are regulated by Notch3. Interestingly, the most strongly enriched pathway in the Notch3-correlated gene set is 'cholesterol homeostasis', and 'bile acid metabolism' is also enriched. Cholesterol-derived conjugated bile acids can drive cholangiocarcinoma cell proliferation and cholestasis is a known risk factor for CCA (43, 44) suggesting that part of the effect of Notch3 in CCA could be due to dysregulation of bile acid synthesis and metabolism.

PRH regulates Wnt signalling

PRH over-expression in CCLP1 cells resulted in the differential expression of several genes involved in Wnt signalling including *WNT11*, *WNT16*, *TCF7L1* and the endogenous LRP6

619 inhibitor *DKK1*, and PRH ChIP-seq showed binding of PRH at these loci. These results
620 suggest that PRH directly regulates several key genes in the Wnt signalling pathway. PRH
621 also indirectly promotes Wnt signalling in CCLP1 cells through Notch3-mediated repression
622 of *CDH1*. We infer that the dominant effect of Notch3 on Wnt signalling is to increase the
623 available pool of β–catenin and thus amplify the effects of PRH on Wnt signalling. In
624 addition our PRH over-expression ChIP-seq and RNA-seq data reveal that many EMT-
625 associated genes are direct targets of PRH, including *FAP*, *DST* and *ITGAV*. Thus we
626 conclude that PRH and Notch3 collaborate to drive EMT and Wnt signalling; PRH directly
627 regulates genes that impact on both pathways and indirectly regulates additional genes in the
628 same pathways via Notch3. Macrophages in the tumour microenvironment have been
629 proposed to provide a source of Wnt ligands to drive the dysregulated Wnt signalling
630 observed in CCA (7). We suggest that independently of exogenous Wnts, the Notch3-PRH
631 loop may also drive aberrant autocrine Wnt signalling in CCA.
632 PRH plays a complex role in liver development; PRH null mice are embryonic lethal (45)
633 with multiple defects including defective liver development, decreased proliferation and
634 migration of hepatic progenitors (46, 47). Conditional deletion of PRH (FoxA3-Cre) results
635 in liver hypoplasia and loss of extrahepatic ducts, whereas a later conditional deletion (Alfp-
636 Cre) results in viable mice with cystic ducts and decreased differentiated intrahepatic bile
637 ducts (48). Here we show that PRH protein expression is turned off in mature human bile
638 ducts and that its re-expression in bile duct epithelial cells promotes cell proliferation and cell
639 invasion. One possibility is that the aberrant expression of PRH in differentiated adult bile
640 duct cells mimics the role that PRH plays in promoting tissue growth in early organogenesis
641 as the PRH partners that are required for PRH dependent bile duct differentiation are likely
642 limiting.
643

644

645

646 *PRH and response to chemotherapeutics*

647 We have shown that PRH influences resistance to canonical Wnt pathway inhibition by
648 ICG-001 (an inhibitor of β–catenin acetylation by CBP). As ICG-001 is reported to be
649 effective at reducing tumour growth in a mouse model of CCA carcinogenesis (7) and is in
650 clinical trial for various solid tumours (49), it could become a compound of interest in the
651 development of novel CCA treatments. Our data suggests that in this case, patient
652 stratification on the basis of PRH expression may be useful to optimise the clinical benefits of
653 this drug or its future derivatives. Inhibition of Notch signalling by targeting the γ-secretase
654 complex is an emerging chemotherapeutic strategy for a variety of cancers (71 clinical trials
655 undertaken as of 2018 (50)). Our data suggests that as well as driving aberrant Notch
656 signalling, PRH also determines resistance to Notch inhibition, at least by non-transition state
657 analogue γ-secretase inhibitors such as DAPT. Our Notch3 knockdown data suggests that
658 direct targeting of Notch3 (for example, by a blocking antibody or by a small molecule that
659 specifically interrupts interactions between Notch3-ICD and components of the Notch
660 transcriptional complex) could be more effective than γ-secretase inhibition. In addition, the
661 CDK4/6 inhibitor palbociclib strongly inhibited the proliferation of CCA cells in the presence
662 of exogenous PRH whereas it had significantly less effect on control cells at the same
663 concentration and PRH knockdown cells were resistant to pablociclib treatment. The effects
664 of palbociclib on CCA cells are thought to be dependent on Rb expression and it is interesting
665 to note that primary BECs and immortalised BECs express much lower levels of Rb than
666 CCA cell lines. Moreover, the effects of palbociclib on CCLP1 cells are largely lost in the
667 absence of Rb and are abolished when PRH is knocked down. These data suggest that CCA
668 cells with high PRH are likely to be highly sensitive to palbociclib treatment and that this

669 sensitivity is driven by the presence of PRH in these cells, but also requires Rb. These data
670 also indicate that at least part of the mechanism by which PRH drives cell proliferation is
671 likely to be through hyper-activation of CDK4/6. We show that PRH activates cyclin D2
672 expression via Notch3 and directly represses *CDKN2B* (p27) and *CDKN1B* (p15). Moreover
673 these data suggest that palbociclib or other CDK4/6 specific inhibitors could be especially
674 effective in the treatment of CCA with high PRH expression levels.
675 In conclusion, we propose that monitoring PRH and Notch3 levels in patients with high CCA
676 risk biliary pathologies, either directly by biopsy or indirectly by detection of the protein
677 products of a set of PRH/Notch3 transcriptional targets (such as cell surface proteins or
678 secreted proteins) in bile or serum may be a useful diagnostic tool to help predict the
679 development of CCA in at-risk groups such as PSC patients in the West and liver fluke-
680 infected patients in south-east Asia. In addition, monitoring PRH expression in patients with
681 CCA may be a useful tool for guiding the choice of chemotherapeutic strategy.

682 **Acknowledgments**

683 We would like to thank Ms L. Wallace for technical assistance isolating primary BECs, Dr
684 Anetta Ptasinska for help with the ChIP protocol and Ms Gagandeep Batth for Akt Western
685 blotting experiments. We thank Prof. Constanze Bonifer for comments on the manuscript and
686 for providing palbociclib and Dr John Halsall for UNC1999. We also thank Prof. Stefan
687 Roberts (University of Bristol) for critical reading of this manuscript and useful discussions.
688 This work was funded by an MRC Newton Fund Project Grant (MR/N012615/1) and
689 Thailand Research Fund (TRF) (DBG5980005).

690

References

1 Bridgewater et al. PRG, , Shahid A. Khan, Josep M. Llovet, , Joong-Won Park Tushar Patel, Timothy M. Pawlik, Gregory J. Gores. Guidelines for the diagnosis and management of intrahepatic cholangiocarcinoma. *journal of Hepatology* 2014; 60: 1268-1289.

2 Landskron G, De la Fuente M, Thuwajit P, Thuwajit C, Hermoso MA. Chronic inflammation and cytokines in the tumor microenvironment. *J Immunol Res* 2014; 2014: 149185.

3 Ye X, Weinberg RA. Epithelial-Mesenchymal Plasticity: A Central Regulator of Cancer Progression. *Trends in cell biology* 2015; 25: 675-686.

4 Takebe N, Warren RQ, Ivy SP. Breast cancer growth and metastasis: interplay between cancer stem cells, embryonic signaling pathways and epithelial-to-mesenchymal transition. *Breast cancer research : BCR* 2011; 13: 211.

5 Polyak K, Weinberg RA. Transitions between epithelial and mesenchymal states: acquisition of malignant and stem cell traits. *Nature reviews Cancer* 2009; 9: 265-273.

6 Cardinale V, Renzi A, Carpino G, Torrice A, Bragazzi MC, Giuliante F *et al*. Profiles of cancer stem cell subpopulations in cholangiocarcinomas. *The American journal of pathology* 2015; 185: 1724-1739.

7 Boulter L, Guest RV, Kendall TJ, Wilson DH, Wojtacha D, Robson AJ *et al*. WNT signaling drives cholangiocarcinoma growth and can be pharmacologically inhibited. *The Journal of clinical investigation* 2015; 125: 1269-1285.

8 Guest RV, Boulter L, Dwyer BJ, Forbes SJ. Understanding liver regeneration to bring new insights to the mechanisms driving cholangiocarcinoma. *NPJ Regen Med* 2017; 2: 13.

9 Loilome W, Bungkanjana P, Techasen A, Namwat N, Yongvanit P, Puapairoj A *et al*. Activated macrophages promote Wnt/beta-catenin signaling in cholangiocarcinoma cells. *Tumour biology : the journal of the International Society for Oncodevelopmental Biology and Medicine* 2014; 35: 5357-5367.

10 Guest RV, Boulter L, Dwyer BJ, Kendall TJ, Man TY, Minnis-Lyons SE *et al*. Notch3 drives development and progression of cholangiocarcinoma. *Proc Natl Acad Sci U S A* 2016; 113: 12250-12255.

11 Geisler F, Strazzabosco M. Emerging roles of Notch signaling in liver disease. *Hepatology* 2015; 61: 382-392.

12 Boulter L, Govaere O, Bird TG, Radulescu S, Ramachandran P, Pellicoro A *et al*. Macrophage-derived Wnt opposes Notch signaling to specify hepatic progenitor cell fate in chronic liver disease. *Nature medicine* 2012; 18: 572-579.

13 Gaston K, Tsitsilianos MA, Wadey K, Jayaraman PS. Misregulation of the proline rich homeodomain (PRH/HHEX) protein in cancer cells and its consequences for tumour growth and invasion. *Cell & bioscience* 2016; 6: 12.

14 Zong Y, Stanger BZ. Molecular mechanisms of bile duct development. *Int J Biochem Cell Biol* 2011; 43: 257-264.

15 Bhave VS, Mars W, Donthamsetty S, Zhang X, Tan L, Luo J *et al*. Regulation of liver growth by glypican 3, CD81, hedgehog, and Hhex. *The American journal of pathology* (Research Support, N.I.H., Extramural) 2013; 183: 153-159.

16 Su J, You P, Zhao JP, Zhang SL, Song SH, Fu ZR *et al*. A potential role for the homeoprotein Hhex in hepatocellular carcinoma progression. *Med Oncol* (Comparative Study

Research Support, Non-U.S. Gov't) 2012; 29: 1059-1067.

17 Marfil V, Blazquez M, Serrano F, Castell JV, Bort R. Growth-promoting and tumourigenic activity of c-Myc is suppressed by Hhex. *Oncogene* (Research Support, Non-U.S. Gov't) 2015; 34: 3011-3022.

18 Kershaw RM, Siddiqui YH, Roberts D, Jayaraman PS, Gaston K. PRH/HHex inhibits the migration of breast and prostate epithelial cells through direct transcriptional regulation of Endoglin. *Oncogene* 2014; 33: 5592-5600.
19 Siddiqui YH, Kershaw RM, Humphreys EH, Assis Junior EM, Chaudhri S, Jayaraman PS *et al*. CK2 abrogates the inhibitory effects of PRH/HHEX on prostate cancer cell migration and invasion and acts through PRH to control cell proliferation. *Oncogenesis* 2017; 6: e293.
20 Kershaw RM, Roberts D, Wragg J, Shaaban AM, Humphreys E, Halsall J *et al*. Proline-Rich Homeodomain protein (PRH/HHEX) is a suppressor of breast tumour growth. *Oncogenesis* 2017; 6: e346.
21 Smith S, Tripathi R, Goodings C, Cleveland S, Mathias E, Hardaway JA *et al*. LIM Domain Only-2 (LMO2) Induces T-Cell Leukemia by Two Distinct Pathways. *PloS one* 2014; 9.
22 McCormack MP, Young LF, Vasudevan S, de Graaf CA, Codrington R, Rabbitts TH *et al*. The Lmo2 oncogene initiates leukemia in mice by inducing thymocyte self-renewal. *Science* 2010; 327: 879-883.
23 Shields BJ, Jackson JT, Metcalf D, Shi W, Huang Q, Garnham AL *et al*. Acute myeloid leukemia requires Hhex to enable PRC2-mediated epigenetic repression of Cdkn2a. *Genes Dev* 2016; 30: 78-91.
24 Zamparini AL, Watts T, Gardner CE, Tomlinson SR, Johnston GI, Brickman JM. Hex acts with beta-catenin to regulate anteroposterior patterning via a Groucho-related co-repressor and Nodal. *Development* 2006; 133: 3709-3722.
25 Marfil V, Moya M, Pierreux CE, Castell JV, Lemaigre FP, Real FX *et al*. Interaction between Hhex and SOX13 modulates Wnt/TCF activity. *JBiolChem* (M109.046649 pii ;10.1074/jbc.M109.046649 doi) 2010; 285: 5726-5737.
26 Nussler AK, Vergani G, Gollin SM, Dorko K, Morris SM, Jr., Demetris AJ *et al*. Isolation and characterization of a human hepatic epithelial-like cell line (AKN-1) from a normal liver. *In vitro cellular & developmental biology Animal* 1999; 35: 190-197.
27 Shimizu Y, Demetris AJ, Gollin SM, Storto PD, Bedford HM, Altarac S *et al*. Two new human cholangiocarcinoma cell lines and their cytogenetics and responses to growth factors, hormones, cytokines or immunologic effector cells. *International journal of cancer Journal international du cancer* 1992; 52: 252-260.
28 Sripa B, Leungwattanawanit S, Nitta T, Wongkham C, Bhudhisawasdi V, Puapairoj A *et al*. Establishment and characterization of an opisthorchiasis-associated cholangiocarcinoma cell line (KKU-100). *World journal of gastroenterology : WJG* 2005; 11: 3392-3397.
29 Sirisinha S, Tengchaisri T, Boonpucknavig S, Prempracha N, Ratanarapee S, Pausawasdi A. Establishment and characterization of a cholangiocarcinoma cell line from a Thai patient with intrahepatic bile duct cancer. *Asian Pac J Allergy Immunol* 1991; 9: 153-157.
30 Rattanasinganchan P, Leelawat K, Treepongkaruna SA, Tocharoentanaphol C, Subwongcharoen S, Suthiphongchai T *et al*. Establishment and characterization of a cholangiocarcinoma cell line (RMCCA-1) from a Thai patient. *World journal of gastroenterology : WJG* 2006; 12: 6500-6506.
31 Lleo A, Zhang W, McDonald WH, Seeley EH, Leung PS, Coppel RL *et al*. Shotgun proteomics: identification of unique protein profiles of apoptotic bodies from biliary epithelial cells. *Hepatology* 2014; 60: 1314-1323.
32 Desjobert C, Noy P, Swingler T, Williams H, Gaston K, Jayaraman PS. The PRH/Hex repressor protein causes nuclear retention of Groucho/TLE co-repressors. *The Biochemical journal* (Research Support, Non-U.S. Gov't) 2009; 417: 121-132.
33 Jayaraman P, Frampton J, Goodwin G. The homeodomain protein PRH influences the differentiation of haematopoietic cells. *LeukRes* 2000; 24: 1023-1031.
34 Noy P, Sawasdichai A, Jayaraman PS, Gaston K. Protein kinase CK2 inactivates PRH/Hhex using multiple mechanisms to de-repress VEGF-signalling genes and promote cell survival. *Nucleic Acids Res* 2012; 40: 9008-9020.

35 Borowicz S, Van Scoyk M, Avasarala S, Karuppusamy Rathinam MK, Tauler J, Bikkavilli RK *et al*. The soft agar colony formation assay. *Journal of visualized experiments : JoVE* 2014: e51998.
36 Liberzon A, Birger C, Thorvaldsdottir H, Ghandi M, Mesirov JP, Tamayo P. The Molecular Signatures Database (MSigDB) hallmark gene set collection. *Cell Syst* 2015; 1: 417-425.
37 Manning BD, Toker A. AKT/PKB Signaling: Navigating the Network. *Cell* 2017; 169: 381-405.
38 Crompton MR, Bartlett TJ, MacGregor AD, Manfioletti G, Buratti E, Giancotti V *et al*. Identification of a novel vertebrate homeobox gene expressed in haematopoietic cells. *Nucleic Acids Res* 1992; 20: 5661-5667.
39 Williams H, Jayaraman PS, Gaston K. DNA wrapping and distortion by an oligomeric homeodomain protein. *JMolBiol* 2008; 383: 10-23.
40 Korinek V, Barker N, Morin PJ, van Wichen D, de Weger R, Kinzler KW *et al*. Constitutive transcriptional activation by a beta-catenin-Tcf complex in APC-/- colon carcinoma. *Science* 1997; 275: 1784-1787.
41 Bienz M. beta-Catenin: a pivot between cell adhesion and Wnt signalling. *Current biology : CB* 2005; 15: R64-67.
42 Knudsen ES, Hutcheson J, Vail P, Witkiewicz AK. Biological specificity of CDK4/6 inhibitors: dose response relationship, in vivo signaling, and composite response signature. *Oncotarget* 2017; 8: 43678-43691.
43 Liu R, Zhao R, Zhou X, Liang X, Campbell DJ, Zhang X *et al*. Conjugated bile acids promote cholangiocarcinoma cell invasive growth through activation of sphingosine 1-phosphate receptor 2. *Hepatology* 2014; 60: 908-918.
44 Lozano E, Sanchez-Vicente L, Monte MJ, Herraez E, Briz O, Banales JM *et al*. Cocarcinogenic effects of intrahepatic bile acid accumulation in cholangiocarcinoma development. *Molecular cancer research : MCR* 2014; 12: 91-100.
45 Hallaq H, Pinter E, Enciso J, McGrath J, Zeiss C, Brueckner M *et al*. A null mutation of Hhex results in abnormal cardiac development, defective vasculogenesis and elevated Vegfa levels. *Development* 2004; 131: 5197-5209.
46 Bort R, Martinez-Barbera JP, Beddington RS, Zaret KS. Hex homeobox gene-dependent tissue positioning is required for organogenesis of the ventral pancreas. *Development* 2004; 131: 797-806.
47 Bort R, Signore M, Tremblay K, Martinez Barbera JP, Zaret KS. Hex homeobox gene controls the transition of the endoderm to a pseudostratified, cell emergent epithelium for liver bud development. *DevBiol* 2006; 290: 44-56.
48 Hunter MP, Wilson CM, Jiang X, Cong R, Vasavada H, Kaestner KH *et al*. The homeobox gene Hhex is essential for proper hepatoblast differentiation and bile duct morphogenesis. *DevBiol* 2007; 308: 355-367.
49 Lyou Y, Habowski AN, Chen GT, Waterman ML. Inhibition of nuclear Wnt signalling: challenges of an elusive target for cancer therapy. *Br J Pharmacol* 2017; 174: 4589-4599.
50 Tamagnone L, Zacchigna S, Rehman M. Taming the Notch Transcriptional Regulator for Cancer Therapy. *Molecules* 2018; 23.

Figure legends

Figure 1 PRH is over-expressed in cholangiocarcinoma.

(A) Representative immunostaining of PRH in a cholangiocarcinoma tissue microarray. Arrowheads mark border tissue biliary epithelium. (B) Quantification of PRH staining intensity in non-involved bile ducts compared to cholangiocarcinoma. (C) Western blot showing PRH expression in four human cholangiocarcinoma cell lines, two human primary biliary epithelial cell isolates and an immortalised cholangiocyte cell line. (D) Growth of CCLP1 control (34±17 mm^3) and PRH knockdown tumours (176±27 mm^2) in nude mouse xenografts, n=9 per group, p=0.0006 at day 25. (E) Proportion of colony initiating cells in soft agar for PRH knockdown (3.4±0.4%) and control (7.6±0.5%) CCLP1 cells, n=3, p=0.01. (F) Final cross-sectional area of colonies in soft agar for PRH knockdown (2063±103 μm^2) and control (4783±53 μm^2) CCLP1 cells, n=3, p=0.002. (G, H) As E,F for AKN1 cells. (I) Colony formation in soft agar of primary BECs infected with Ad myc-PRH or empty adenovirus. *denotes $p<0.05$.

Figure 2 Effects of PRH manipulation on cholangiocarcinoma cell biology.

(A) Proliferation of CCLP1 cells stably transfected with PRH shRNA or scrambled control, n=3, p=0.03. (B) Proliferation of CCLP1 and CCSW1 cells infected with Ad myc-PRH or empty virus control, n=3, p=0.03 (CCLP1), p=0.02 (CCSW1). (C) Proliferation of AKN1 and primary BECs over-expressing GFP-PRH-myc (stable) or myc-PRH (transient, 48 hours) n=3, p=0.003 (AKN1), p=0.006 (BEC). (D) Morphology of CCLP1 cells stably transfected with PRH shRNA or scrambled control. (E) Western blot showing increased expression of E-cadherin protein after PRH knockdown. Lamin A/C as loading control. (F) Migration of CCLP1 PRH knockdown cells through transwell filters in a 10% serum gradient, n=3, p=0.03. (G) Invasion of CCLP1 cells through Matrigel, n=4, p=0.03. (H) Western blotting for

857 myc-PRH and EMT associated proteins E-cadherin and Vimentin in AKN1 cells and primary
858 BECs. (I,J) As G,H for AKN1 cells and primary BECs. *denotes $p<0.05$. (K) Morphology of
859 equal numbers of AKN1 cells stably transfected with plasmids expressing GFP (control) or a
860 GFP-PRH-Myc-tagged fusion protein (GFP-PRH-Myc). The scale bars represent 50 μM in
861 length.
862
863 **Figure 3 RNA sequencing of PRH knockdown and over-expressing CCLP1 cells.**
864 (A) Number of differentially expressed genes (DEGs) detected in PRH knockdown (KD) and
865 over-expression (OE) experiments, and overlap of these gene sets. (B,C) GSEA using
866 Hallmark gene sets for PRH OE and KD DEGs. Red bars represent Hallmark sets that are
867 enriched in both PRH KD and OE DEG lists. FDR – false discovery rate. (D) log2 fold
868 change of gene expression from PRH OE and KD RNA-seq for BEC related genes. TF -
869 transcription factor.
870
871 **Figure 4 Notch3 expression is regulated by PRH.**
872 (A) Western blot showing Notch3 protein expression in PRH knockdown CCLP1 cells. (B)
873 *NOTCH3* gene expression in CCLP1 and CCSW1 cells infected with Ad myc-PRH, Ad myc-
874 PRH DNA-binding deficient N187A mutant or empty virus control. (C) Western blot for
875 CCLP1 samples in panel B. (D) Notch3 protein expression correlates with PRH protein
876 expression in four human cholangiocarcinoma cell lines, two human primary biliary epithelial
877 cell isolates and an immortalised BEC line. (E) Western blot showing elevated expression of
878 Notch3 upon PRH over-expression in both AKN1 cells and primary BECs. (F) Western blot
879 showing increased expression of E-cadherin and reduced expression of PRH proteins after
880 Notch3 knockdown. Lamin A/C as loading control. (G) Proliferation of CCLP1 cells stably
881 transfected with Notch3 shRNA or scrambled control, n=3, p=0.04. (H) Morphology of

CCLP1 cells stably transfected with Notch3 shRNA or scrambled control. (I) DEGs detected in Notch3 KD compared to PRH KD experiments. Hypergeometric test $p=10^{-229}$ for up-regulated genes and $p=10^{-31}$ for down-regulated genes. (J) Hallmark GSEA of genes differentially expressed after Notch3 KD. Red bars indicate gene sets that are also enriched after PRH knockdown.

Figure 5 Notch3- and PRH-correlated gene sets.

(A) qRT-PCR analysis of genes from CCLP1 cells over-expressing PRH in the presence or absence of Notch3 shRNA identifying PRH and Notch3 correlated expression signatures. (B) Western blot analysis of EMT proteins E-cadherin and Vimentin and Cyclin D2 in CCLP1 cells over-expressing myc-PRH in the presence of absence of Notch3 shRNA. (C) Proliferation of CCLP1 cells over-expressing myc-PRH in the presence or absence of Notch3 shRNA. (D) Hallmark GSEA of Notch3-correlated and PRH correlated gene sets identified from analysis of RNA-seq data. Red bars indicate gene sets enriched in both PRH- and Notch3-correlated sets. * denotes $p<0.05$ after Bonferroni correction, compared to non-targeting shRNA/empty virus control. # denotes no statistically significant difference in the comparison indicated. (E) Overlap of genes with PRH binding sites determined by ChIP-seq and genes that are differentially expressed after PRH over-expression determined by RNA-seq in CCLP1 cells. (F) Comparison of the primary motif underlying PRH ChIP-seq peaks identified using HOMER with the PRH SELEX motif (derived from (38)). (G) RNA-seq and ChIP-seq tracks of putative direct PRH target *DKK1*. Red tracks indicate myc-PRH over-expression. (H). RNA-seq and ChIP-seq tracks of putative direct PRH target *WNT11*. Red tracks indicate myc-PRH over-expression.

Figure 6 Regulation of Wnt signalling.

(A) TOPFlash TCF/LEF reporter activity in CCLP1 and CCSW1 cells expressing myc-PRH, DNA-binding deficient N187A mutant of myc-PRH and Flag-Notch3-ICD. Inset: Western blot showing expression of myc-PRH constructs. (B) Representative immunofluorescence micrographs of CCLP1 PRH knockdown cells stained for E-cadherin and β-catenin. (C) Western blot of subcellular fractions of CCLP1 PRH knockdown cells. (D) TOPFlash reporter activity in PRH knockdown CCLP1 cells. (E) TOPFlash reporter activity in control CCLP1 cells (pcDNA empty) and CCLP1 cells over-expressing E-cadherin (CDH1) in the presence and absence of myc-PRH expression. Inset: Western blot showing successful over-expression of E-cadherin. *denotes $p<0.05$, # denotes no statistically significant difference.

Figure 7 Altered sensitivity to therapeutics.

(A) Proliferation measured by EdU incorporation in CCLP1 cells infected with Ad empty or Ad myc-PRH and treated with various compounds used at their LD50 as shown (B) Log sensitivity ratio to compounds from panel A. Drugs with a log ratio >0 are less effective after PRH over-expression and *vice versa*. *denotes a log ratio significantly different ($p<0.05$) from 0, # denotes no significant difference. (C) Proliferation measured by EdU incorporation in a panel of CCA cell lines infected with Ad empty or Ad myc-PRH and treated with palbociclib at their LD50. CCLP1, CCSW and KKU-213 (LD50= 100nM) and KKU-100 (LD50=150nM) as in (A) and presented as log sensitivity ratio as in (B) (*denotes $p<0.05$, **denotes $p<0.01$). (D) Three independent control and Rb knockdown CCLP1 cell populations were treated with palbociclib at 100nM and cell proliferation measured using EdU incorporation assays. Inset: Western blot showing successful knockdown of Rb. *denotes $p<0.05$, ns denotes no statistically significant difference. (E) Schematic of pathways affected by PRH in CCA cells and compounds targeting these pathways. Red indicates

compounds whose efficacy is reduced by PRH over-expression and green indicates compounds whose efficacy is increased.

Figure 1

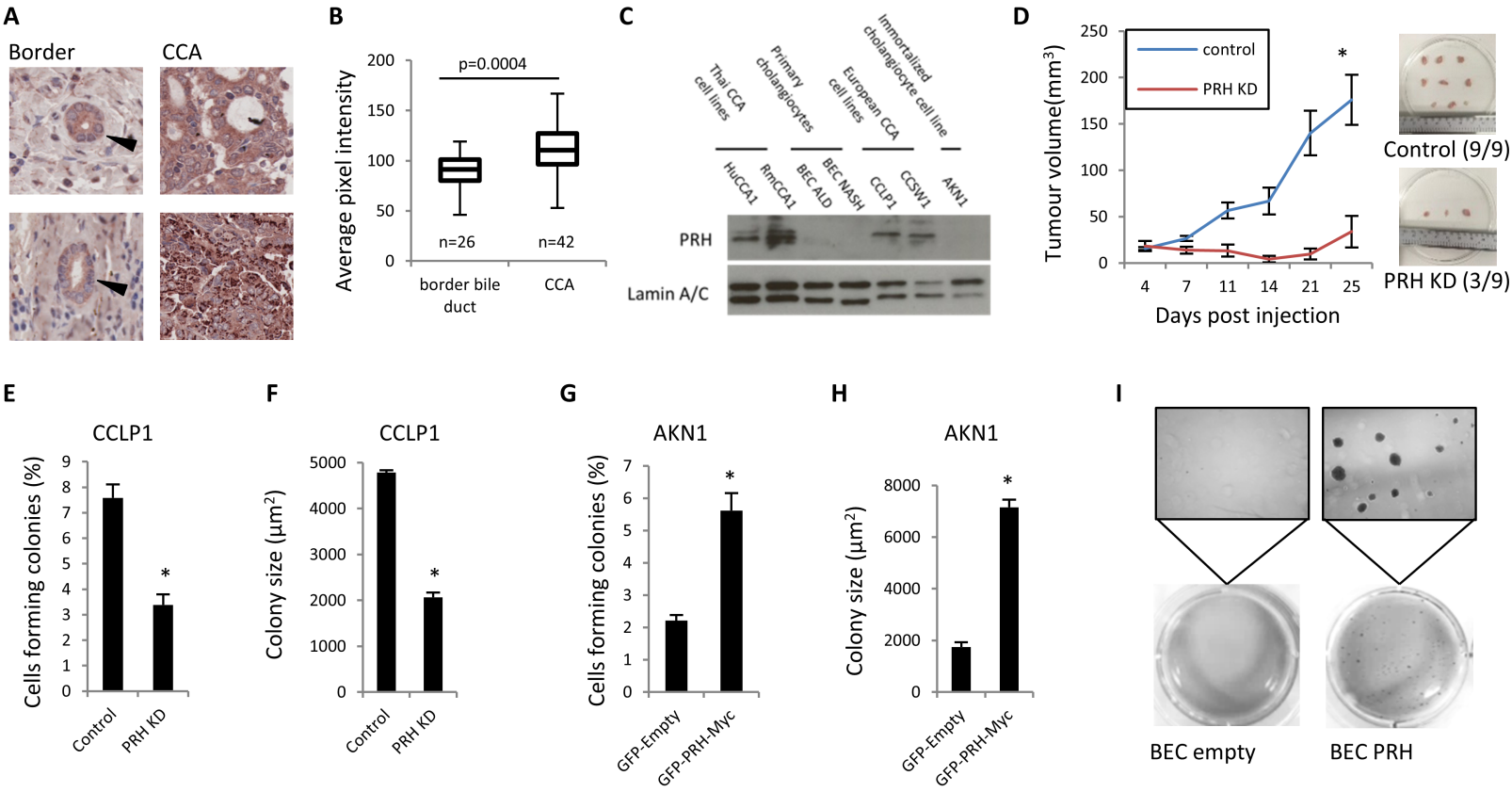

Figure 2

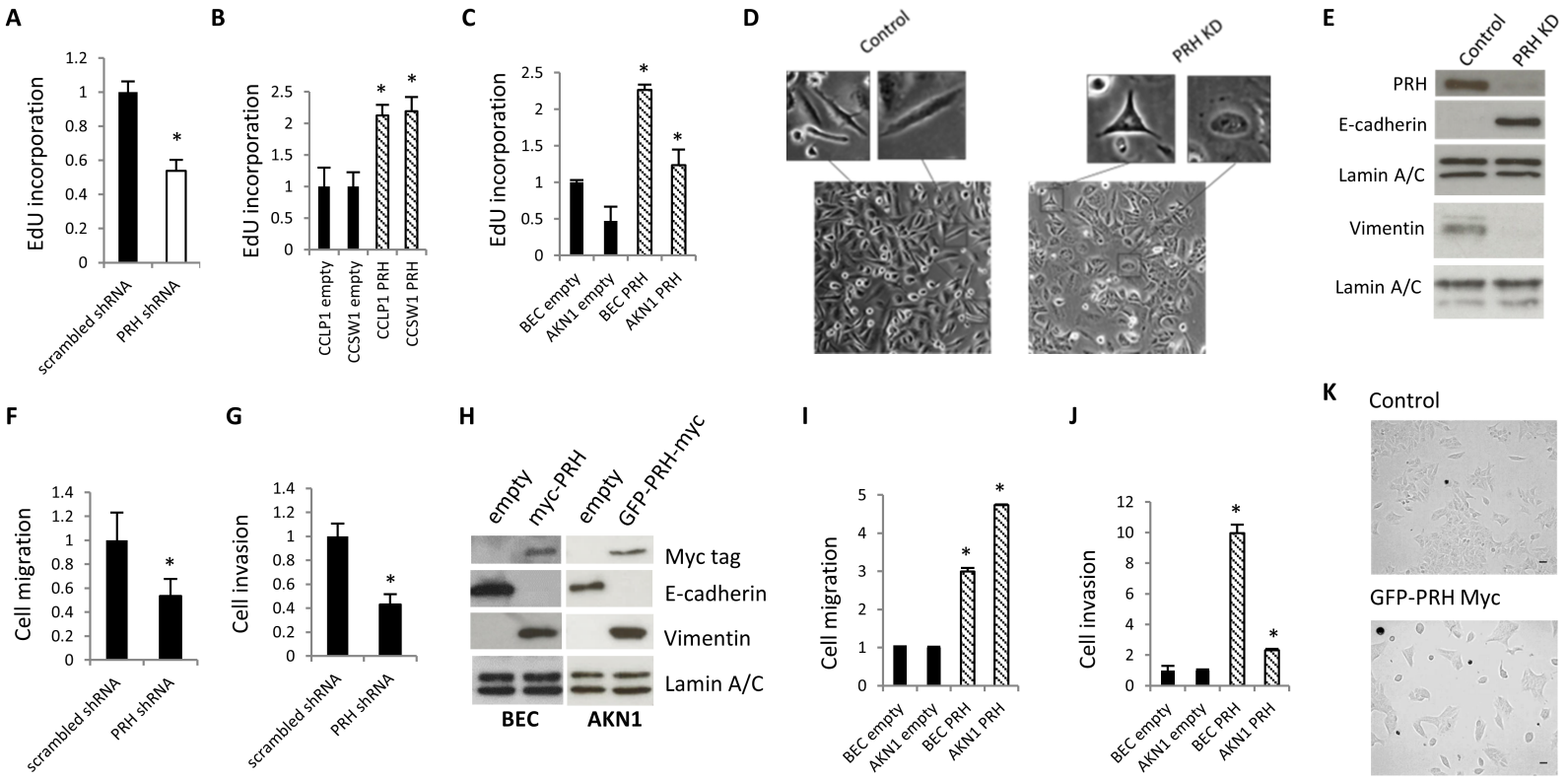

Figure 3

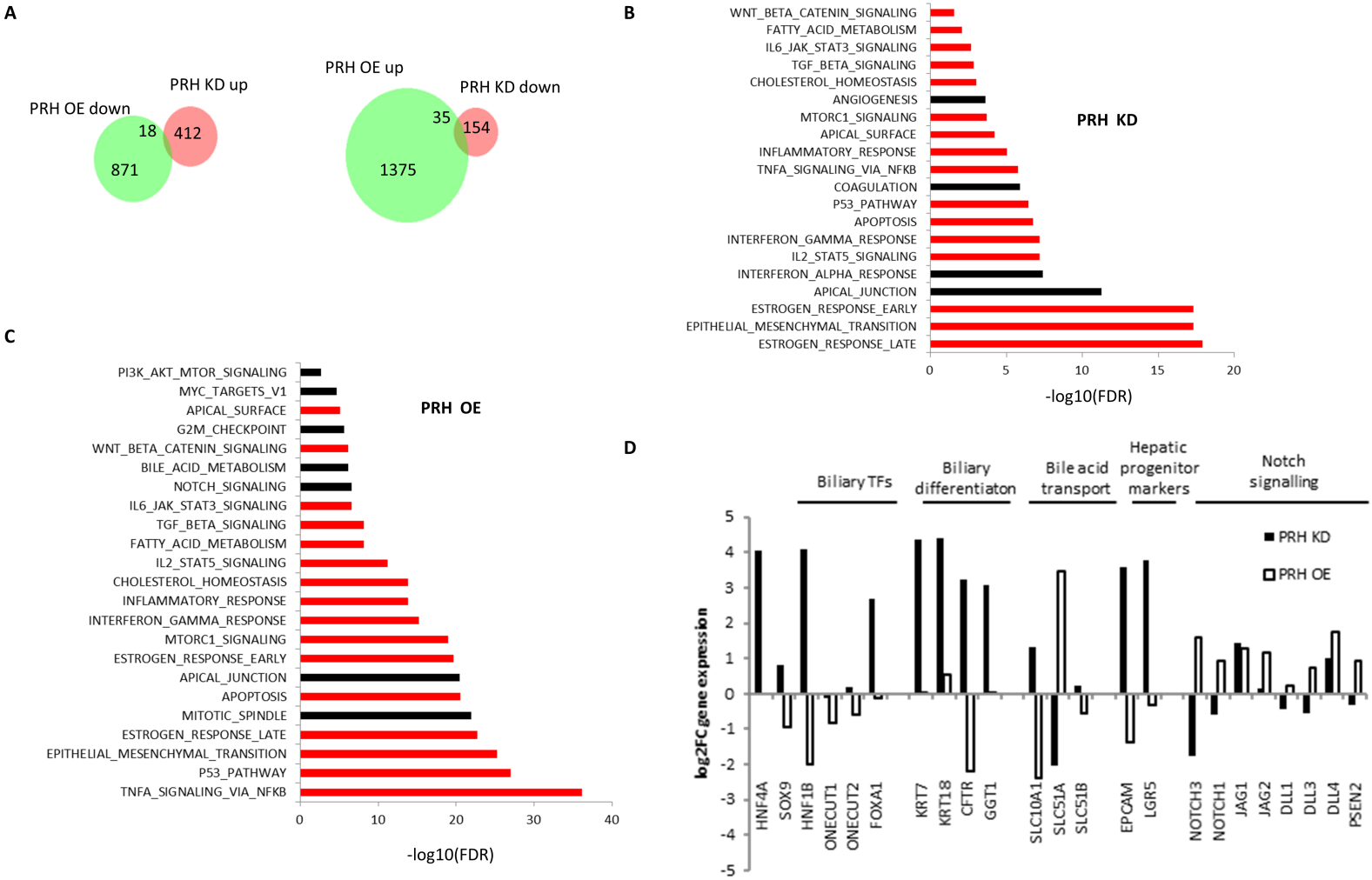

Figure 4

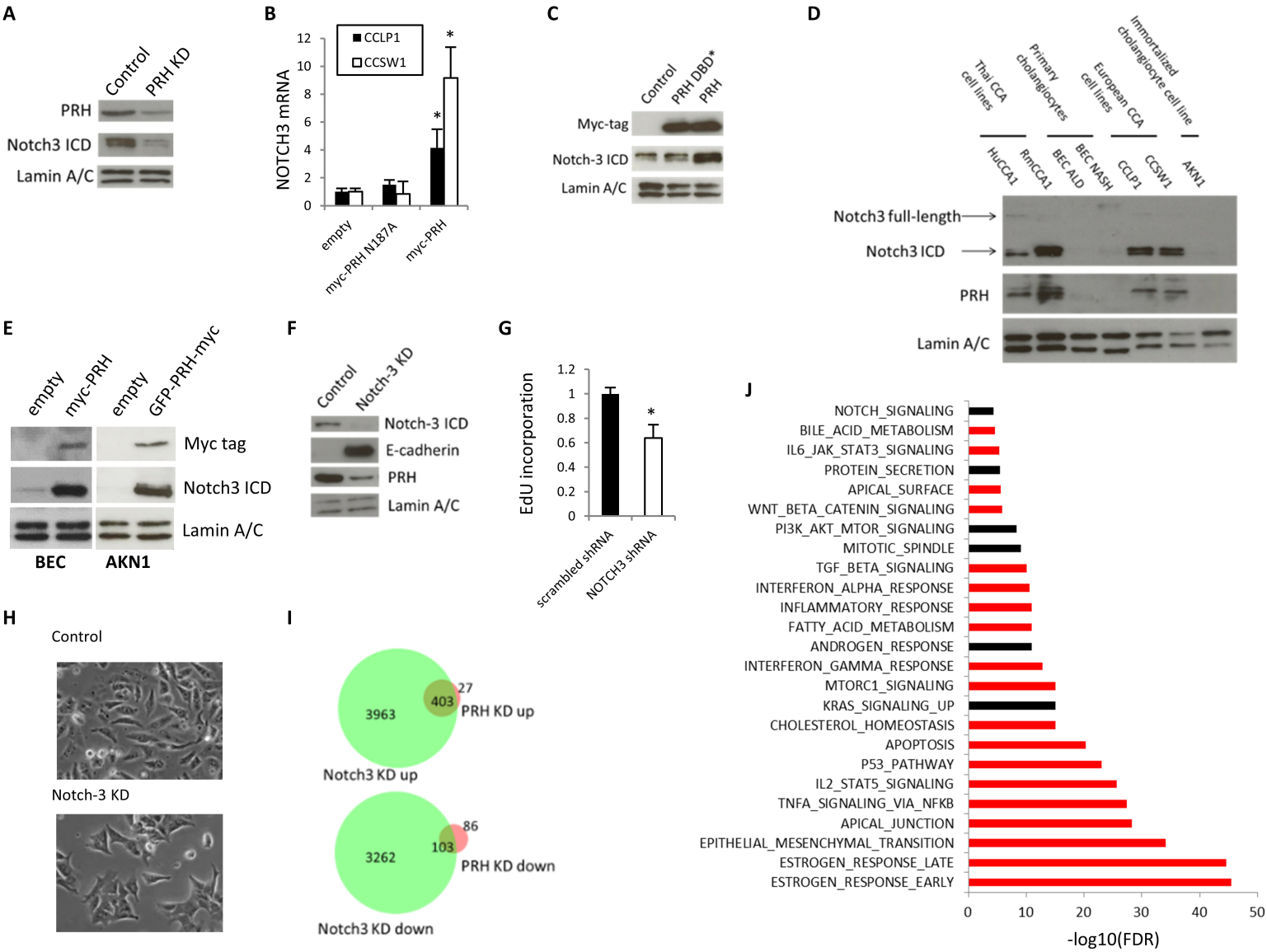

Figure 5

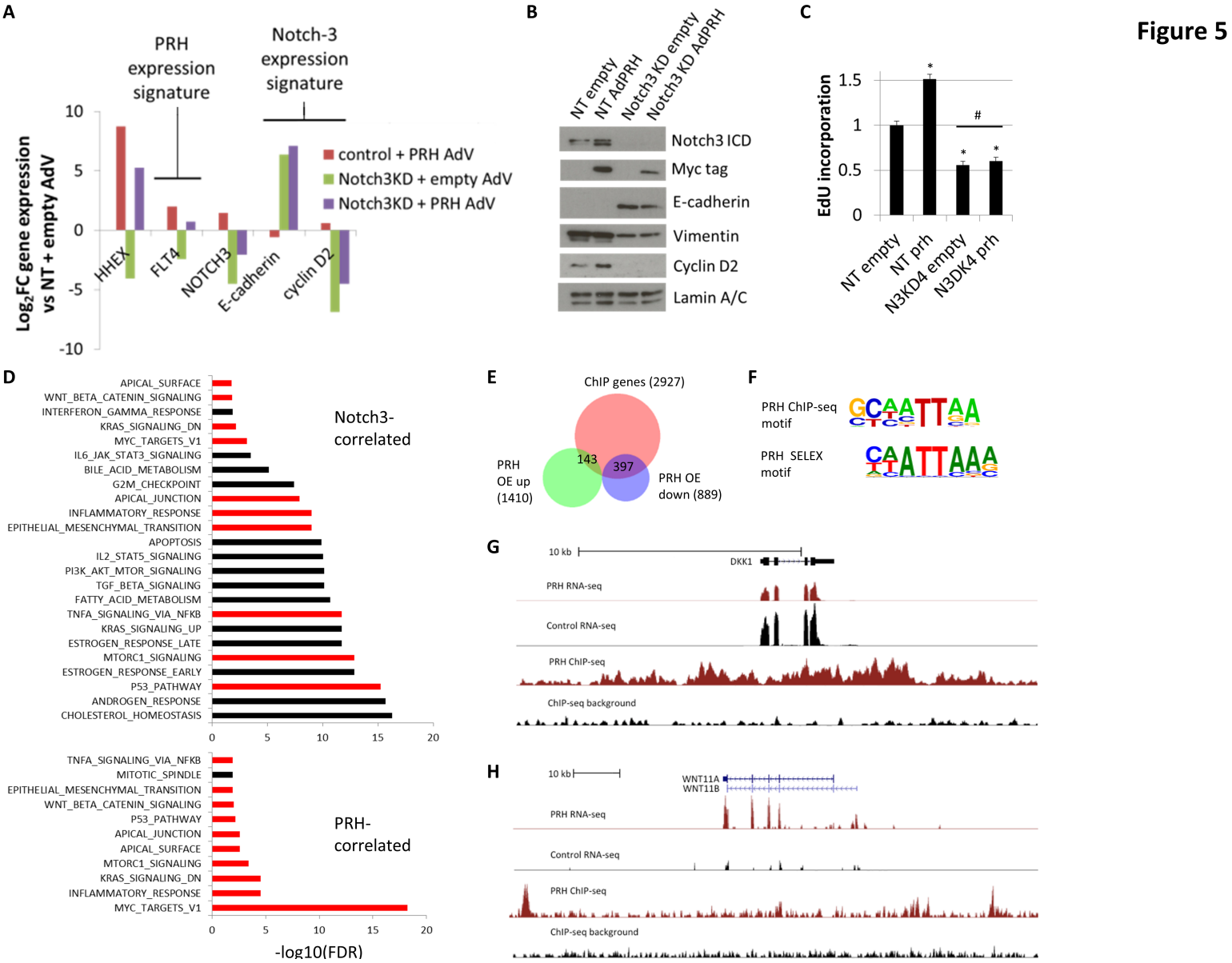

Figure 6

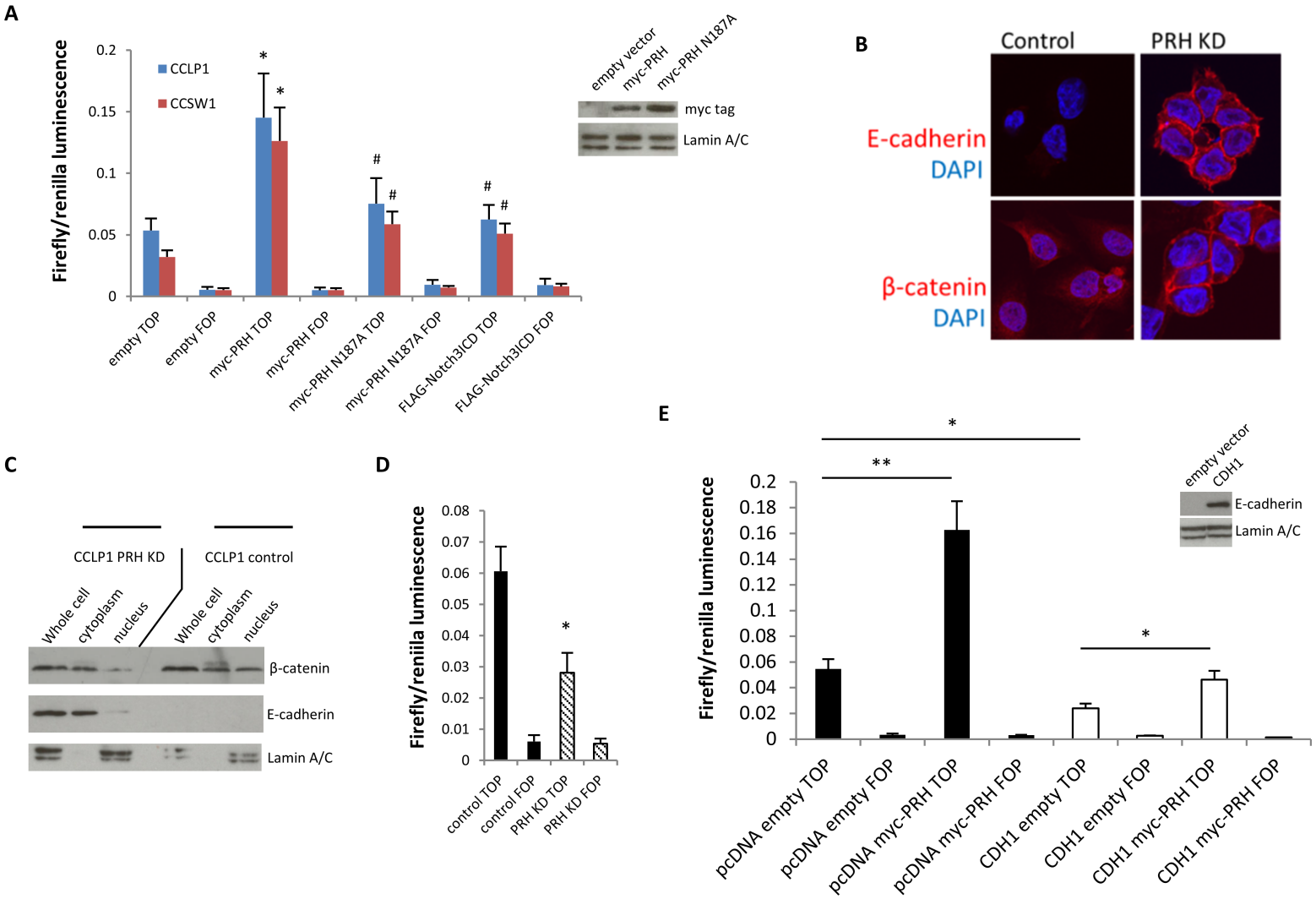

Figure 7

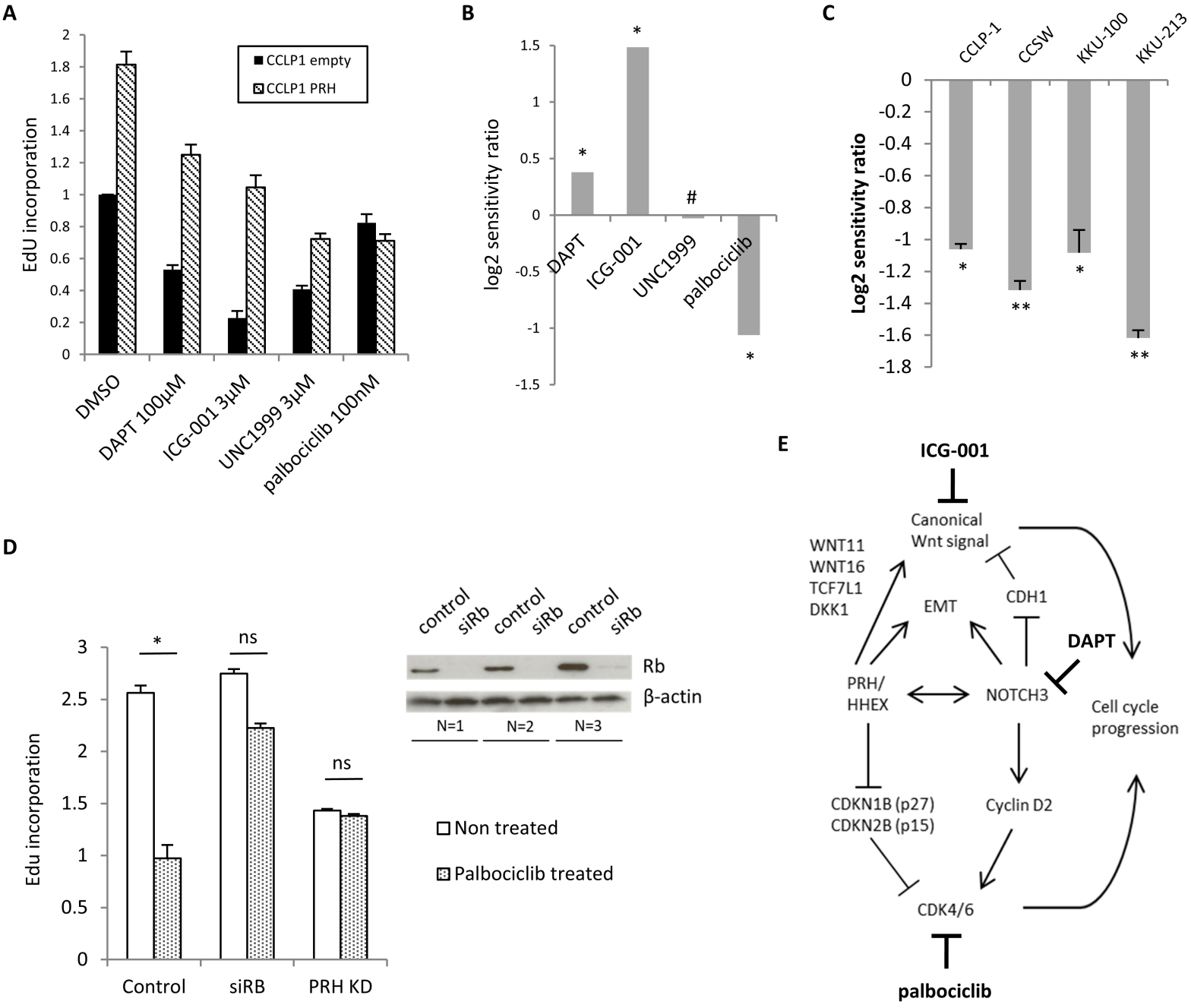

AACR American Association for Cancer Research

Cancer Research

The Journal of Cancer Research (1916–1930) | The American Journal of Cancer (1931–1940)

A runaway PRH/HHEX-Notch3 positive feedback loop drives cholangiocarcinoma and determines response to CDK4/6 inhibition

Philip Kitchen, Ka Ying Lee, Danielle Clark, et al.

Cancer Res Published OnlineFirst December 16, 2019.